Biological, Medical Devices, and Systems

MARIE: A MATLAB-Based Open Source MRI Electromagnetic Analysis Software

J. F. Villena, A. Polimeridis, J. E. C. Serralles, L. Wald, E. Adalsteinsson, J. White, L. Daniel.
Sponsorship: National Institutes of Health, Skoltech Initiative on Computational Mathematics

Our Magnetic Resonance Integral Equation suite (MARIE) is a numerical software platform for comprehensive frequency-domain fast electromagnetic (EM) analysis of MRI systems. The tool is based on a combination of surface and volume integral equation formulations. It exploits the characteristics of the different parts of an MRI system (coil array, shield, and realistic body model), and it applies sophisticated numerical methods to rapidly perform all the required EM simulations to characterize the MRI design: computing the un-tuned coil port parameters, obtaining the current distribution for the tuned coils, and obtaining the corresponding electromagnetic field distribution in the inhomogeneous body for each transmit channel.

The underlying engine of MARIE is based on integral equation methods applied to the different domains that exist in traditional MRI problems (for example, except in interventional cases, the coil and body occupy separate spaces). The natural domain decomposition of the problem allows us to apply and exploit the best modeling engine to each domain. The inhomogeneous human body model is discretized into voxels and modeled by volume integral equation (VIE) methods. The homogeneous conductors that form the coil design and shield are tessellated into surface triangles (that allow the modeling of complex and conformal geometries), and modeled by surface integral equation (SIE) methods. Both models are coupled by applying standard dyadic Green functions. Due to the nature of integral equation methods, there is no need to model or discretize the surrounding air or non-electromagnetic materials, although the solution fields can be computed anywhere outside the discretized domain by applying the same free-space Green functions. Also, no boundary condition needs to be defined (integral equations satisfy the radiation condition by construction), which simplifies the setting of the problem for the user: the inputs are the voxelized definition of the inhomogeneous body model, the tessellated geometry of the coil design (which the external ports defined), and the frequency of operation.

Once the models are generated, fast numerical methods are applied to solve the complete system. A set of nested iterative methods with the appropriate preconditioning is used to solve the effect of each port. Fast Fourier transform (FFT) techniques exploit the regularity of the voxelized grid and accelerate the matrix vector products. Depending on the different scenarios for analysis, some numerical models or tasks can be pre-computed to accelerate the solution, and many strategies are used to reduce either computational time or memory consumption.

The software runs on MATLAB and is able to solve a complex scattering problem in ~2-3 min. on a standard single GPU-accelerated windows desktop machine. On the same platform, it can perform a frequency sweep of a complex coil in ~3-5 min. per frequency point. Furthermore, it can solve the complete inhomogeneous body and coil system in ~5-10 min. per port, depending on the model resolution and error tolerance required. Intended to be a development platform, it includes a simple and intuitive graphic user interface (see Figure 1 for a snapshot) for standard analysis and a set of well-documented scripts to illustrate how to use the core numerical functions to perform more advanced analyses, to allow experienced users to create their own analysis by using or modifying the existing code. The input of the body is voxel-based and can be read from simple files that define position and tissue properties. The input of the coil design is based on standard triangular geometric descriptions, widely popular and with multiple open-source mesh generators available. The underlying numerical routines can be used to generate standard results, such as the B1+, B1-, and E maps presented in Figure 2, or to address other relevant problems, such as the generation of ultimate intrinsic SNR and SAR on realistic body models, fast coil design and optimization, and generation of patient-specific protocols, among others.

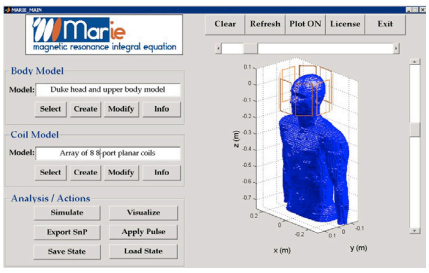

◀ Figure 1: Snapshot of MARIE's graphic user interface with body and coil models loaded, for which the simulation results are shown in Figure 2.

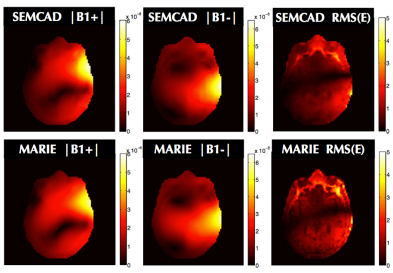

◀ Figure 2: Comparison of the (left) B1+, (center) B1-, and (right) RMS(E) maps for a body model. Top maps are with SEMCAD (SPEAG), bottom with MARIE.

FURTHER READING

- A. G. Polimeridis, J. F. Villena, L. Daniel, and J. K. White, "Stable FFT-JVIE Solvers for Fast Analysis of Highly Inhomogeneous Dielectric Objects," *Journal of Comp. Physics*, vol. 269, pp. 280-296, 2014.
- A. Hochman, J. F. Villena, A. G. Polimeridis, L. M. Silveira, J. K. White, and L. Daniel, "Reduced-order Models for Electromagnetic Scattering Problems," *IEEE Trans. on Antennas and Propagation*, vol. 62, no. 6, pp. 3150-3162, 2014.

Automated Modeling for Large-Scale Arterial Systems

Y.-C. Hsiao, Y. Vassilevski, S. Simakov, L. Daniel
Sponsorship: MIT-Skoltech

Diagnosing medical conditions based on non-invasive (or minimally invasive) measurements requires simultaneous modeling for both (1) local pathological arteries and (2) global arterial networks in order to correlate the available measurements with the actual pathologies. For instance, diagnosing atherosclerosis or an aneurysm requires detailed understanding of the pressure and flow inside the bifurcation segments. Such information is typically not measurable at pathological sites but may still be attainable if it can be inferred from other measurements. Therefore, it is crucial to develop accurate yet efficient global arterial models such that the correlations between the pathologies and the available measurements can be established. The final diagnosis can be obtained by solving an inverse problem for the pathological parameters, for instance, aneurysm internal diameter, arterial wall thickness, plague stiffness, etc.

For this strategy to be effective, the model for such a large-scale arterial network must be compact, computationally tractable, and field-solver-accurate. We have proposed an innovative technique to automatically generate nonlinear dynamic models using measurement data or simulations results from partial-differential-equation (PDE) solvers, as shown in Figure 1. The generated models are guaranteed numerically stable, both when simulated alone and when interconnected within a network. This stability enables the hierarchical modeling capability, generating models for local sub-networks, such as branches and bifurcations, and interconnecting them to form a global network. An example of such geometry decomposition is demonstrated in Figure 2. This approach allows full exploitation of artery geometries without compromise due to the shape complexity. In addition, because the entire modeling efforts are subdivided into local model generations, the corresponding finite-element problems for generating training data are at a tractable size. Therefore, the fluid dynamics PDEs, such as viscosity and turbulence, can be fully utilized to capture all types of nonlinearities without simplification.

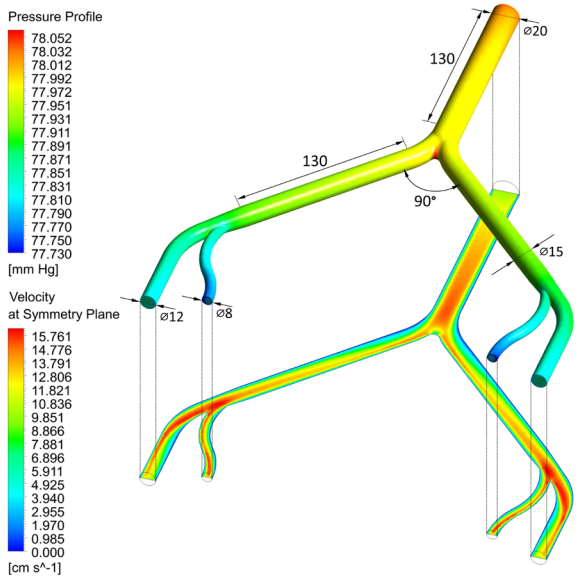

▲ Figure 1: Pressure profile (upper) and velocity profile (lower) of the human abdominal aorta and iliac arteries.

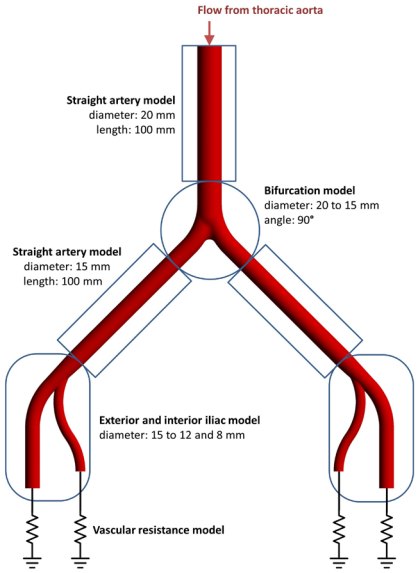

▲ Figure 2: Arterial network decomposition into local models. Each model is automatically generated using our proposed algorithm. The simulation of the overall system is accurate, efficient, and guaranteed numerically stable.

FURTHER READING

- B. Bond, T. Moselhy, and L. Daniel, "System Identification Techniques for Modeling of the Human Arterial System," in *Proc. SIAM Conference on the Life Sciences,* pp. 12-15, 2010.
- Y.-C. Hsiao and L. Daniel, "Sparse Basis Pursuit on Automatic Nonlinear Circuit Modeling," presented at *IEEE International Conference on ASIC (ASICON),* Shenzhen, China.

Three-Dimensional, Magnetic Resonance-Based Electrical Properties Mapping

J. E. C. Serrallés, A. G. Polimeridis, R. Lattanzi, D. K. Sodickson, J. K. White, L. Daniel
Sponsorship: NSF

Over the past few decades, magnetic resonance imaging (MRI) has proven to be a safe and versatile tool in medical practice and clinical research. Clinical MRI typically relies on magnetization, T_1-weighting, and T_2-weighting as its contrast mechanisms. The dependence on these mechanisms is disadvantageous because these quantities are not guaranteed to vary from tissue to tissue, potentially obscuring the true contrast of the tissues. Additionally, the use of magnetization discards valuable information that describes how the scatterer interacts with fields generated by a scanner. The aim of our research is instead to use this extraneous information to generate maps of relative permittivity and of conductivity, thereby significantly increasing contrast in MR images at the expense of computation time.

The task of inferring these material properties is referred to as inverse scattering, a subclass of what are called inverse problems. Inverse scattering problems typically suffer from slow convergence rates and require several full-wave electromagnetic simulations per iteration of the procedure. Our approach, called Global Maxwell Tomography, uses a volume integral equation suite, MARIE, which is custom-tailored for the typical MR setting and which results in runtimes that render inference process tractable. Our algorithm is capable of reconstructing the known electrical properties of objects, in simulation, with use of measured MR data on the horizon. The ability to infer electrical property maps rapidly from MR data would not only improve the reliability of MRI but would also pave the way for applications like automated tumor identification, patient-specific MR shimming, and real-time monitoring of heat deposition in tissue by MR coils, among others.

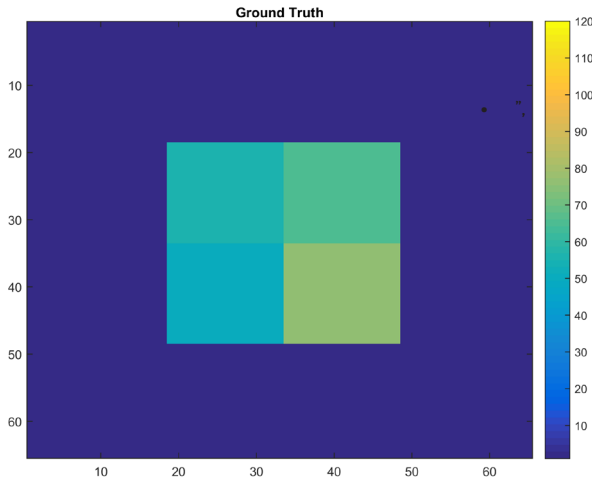

▲ Figure 1: Relative permittivity map of phantom with known electrical properties and geometry, along a central slice. This constitutes the ground truth to which the algorithm should converge.

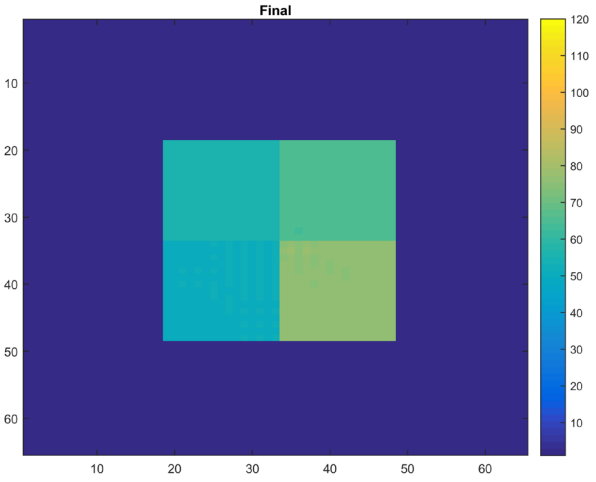

▲ Figure 2: Reconstructed relative permittivity map of the same phantom, when starting from a completely homogeneous initial guess. Reference fields are generated in simulation.

FURTHER READING

- J. E. C. Serrallés, A. G. Polimeridis, M. V. Vaidya, G. Haemer, J.K. White, D.K. Sodickson, L. Daniel, R. Lattanzi. "Global Maxwell Tomography: A Novel Technique for Electrical Properties Mapping without Symmetry Assumptions or Edge Artifacts," presented at *ISMRM 24th Annual Meeting*, Suntec City, Singapore, May 2016.
- J. E. C. Serrallés, L. Daniel, J.K. White, D.K. Sodickson, R. Lattanzi, and A.G. Polimeridis. "Global Maxwell Tomography: A Novel Technique for Electrical Properties Mapping based on MR Measurements and Volume Integral Equation Formulations," presented at *2016 IEEE International Symposium on AP-S–URSI National Radio Science Meeting*, Fajardo, Puerto Rico, June 2016.

A Portable Bioimpedance Spectroscopy Measurement System for Management of Congestive Heart Failure

M. K. Delano, C. G. Sodini
Sponsorship: MEDRC, Analog Devices, Inc.

An estimated five million people are currently diagnosed with congestive heart failure (CHF) in the United States, with over 400,000 new diagnoses annually. Almost one in two patients will be readmitted to the hospital within four to six months of discharge. Readmissions can occur when the patient becomes fluid-overloaded due to poor medication and/or diet compliance, among other reasons. Up to 50% of these early re-admissions may be prevented if symptoms are recognized early enough and medication and diet compliance improve.

CHF is frequently associated with significant fluid retention in the lungs and legs. Bioimpedance techniques can be used to estimate the fluid levels in a patient non-invasively. These measurements have been shown to be predictive of heart failure decompensation up to 14 days before an event occurs.

We have developed a portable bioimpedance system that can measure body impedance from 1 kHz to 1 MHz. The system uses the magnitude-ratio and phase-difference detection (MRPDD) method to calculate the magnitude and phase of the measured impedance (see Figure 1). The system is enclosed in aluminum box (see Figure 2) and can be used with four co-axial cables. Data from the device is transmitted over Bluetooth to an iOS device.

The device has been tested with RC networks and with two healthy participants at MIT's Clinical Research Center. The device will be tested in the hemodialysis unit at Massachusetts General Hospital in 2016.

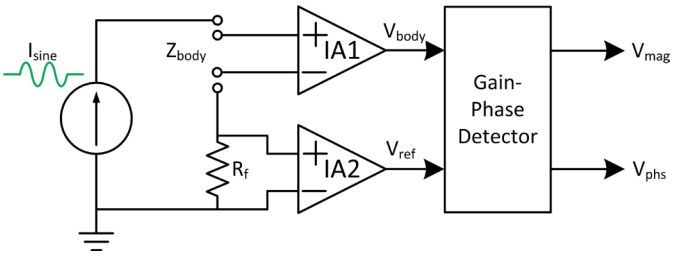

▲ Figure 1: A schematic overview of the MRPDD method. A fixed sinusoidal current is driven through the body and a sense resistor. The voltage is amplified and measured by a gain-phase detector chip (AD8302).

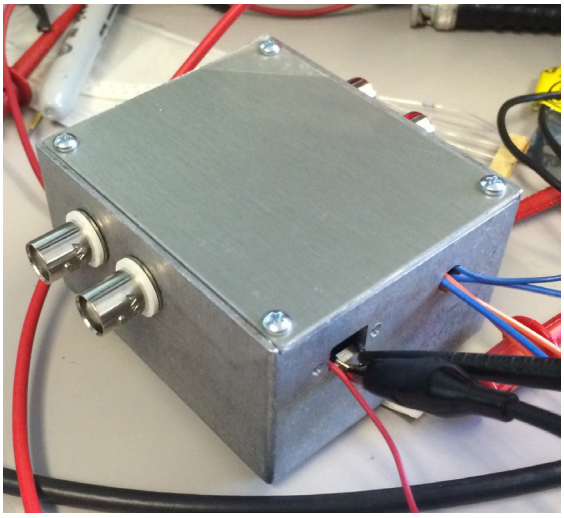

▲ Figure 2: The portable bioimpedance spectroscopy measurement system inside the enclosure.

FURTHER READING

- M. Delano and C. G. Sodini, "A Long Term Wearable Electrocardiogram Measurement System," *Body Sensor Networks Conference*, pp. 1-6, May 2013.
- E. Winokur, M. Delano, and C. G. Sodini, "A Wearable Cardiac Monitor for Long-Term Data Acquisition and Analysis," *IEEE Transactions on Biomedical Engineering*, vol. 60, pp. 189-92, Jan. 2013.
- D. He, E. S. Winokur, and C. G. Sodini, "An Ear-worn Vital Signs Monitor," *IEEE Transactions on Biomedical Engineering*, vol. 62, no. 11, pp. 2547-2552, November 2015.

Body-Coupled Communication and Implants

G. S. Anderson, C. G. Sodini
Sponsorship: Center for Integrated Circuits & Systems

Body-coupled communication (BCC) is achieved by creating a potential difference in one area of the body and sensing the resulting attenuated potential difference in another area of the body. To do this, the transmitter and receiver each have two electrodes that electrically connect to the body's conductive tissues beneath the epidermis. These connections can be formed either capacitively or galvanically. A capacitive link consists of the electrode forming one plate of a parallel plate capacitor while the conductive tissues form the other plate. A galvanic link is formed by directly putting the electrode or wire in the conductive tissue.

For an implant to communicate to a device outside the body using BCC, the channel utilizes both galvanic and capacitive links (capacitive for the device outside the body and galvanic for the implant). To test if this is possible a pork loin was used to simulate the conductive tissue of the body (see Figure 1). First, both the transmitter's and receiver's electrodes were connected to the pork loin using cardboard spacers between the pork loin and the electrodes, ensuring that both the transmitter and receiver would be capacitively coupled to the conductive tissue in the pork loin. Next, the transmitter's output was connected to two alligator clips that were inserted into the pork-loin while the receiver was connected capacitively as before. This configuration simulates an implanted transmitter that is galvanically coupled to the conductive tissue, communicating with a receiver that is capacitively coupled. The results, shown in Figure 2, validate the predictions of the body model detailed in the further reading below.

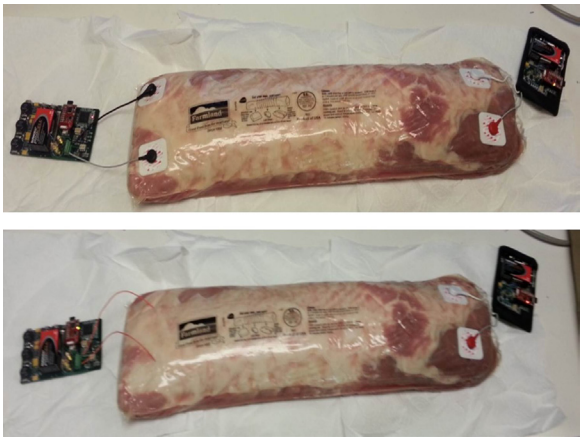

▲ Figure 1: A setup to test implants talking to devices outside the body using BCC.

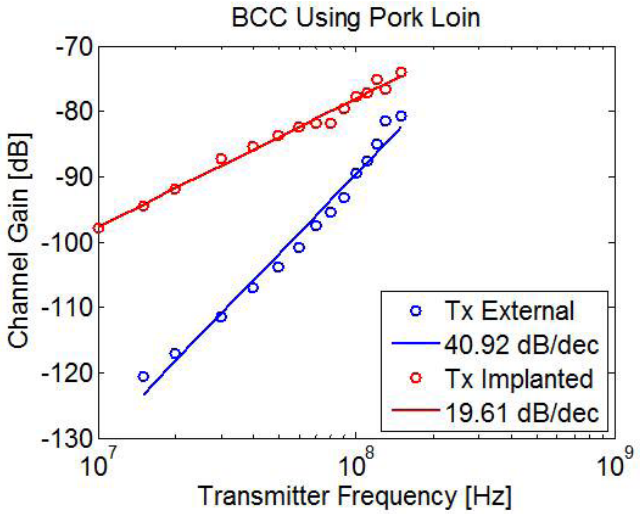

▲ Figure 2: BCC channel measurements.

FURTHER READING

- G. S. Anderson and C. G. Sodini, "Body Coupled Communication: The Channel and Implantable Sensors," *2013 IEEE International Conference on Body Sensor Networks (BSN)*, Cambridge, MA, pp. 1-5, 6-9 May 2013.
- T. G. Zimmerman, "Personal Area Networks (PAN): Near-field Intrabody Communication," *Master's thesis, Massachusetts Institute of Technology*, Cambridge, MA, 1995.
- A. Fazzi *et al*, "A 2.75mW Wideband Correlation-Based Transceiver for Body-Coupled Communication," *ISSCC Dig. Tech. Papers*, pp. 204-205, February 2009.

Miniaturized EEG System and Seizure Detector for Wearable and Subdermal Application

J. Yang, C. G. Sodini
Sponsorship: Center for Integrated Circuits and Systems

Electroencephalograms (EEGs) are used to diagnose and treat a wide range of neurological related topics by providing insight into a patient's brain activity. Their applications range from diagnosing epilepsy and sleep disorders to assisting doctors to administer anesthetic drugs and more.

Achieving long-term continuous EEG data in a wearable form has been a long-standing problem. In a conventional EEG, the patient must go to the hospital and be connected to bulky equipment. This is prohibitively expensive in the long run and prevents the patient from going about their daily lives, thereby reducing patient compliance in certain situations.

This work extends previous investigations on miniaturization of EEG by providing system-level improvements to expand the use-cases of the device. With optimized packaging of an EEG system-on-a chip (SoC) die, form-factors more suitable for implantation as well as wearable designs are realized. For the subdermal implanted design, an eight-channel EEG recorder with a seizure detector is implanted behind a patient's ear. Electrodes are threaded underneath the patient's scalp to the location of interest. EEG data is then sent wirelessly to a wearable external device that processes the data and provides power to the implant. This implantable system has the ability to continuously record EEG for more than 30 days with minimal maintenance.

For the wearable form factor, the miniaturized EEG SoC and wireless microprocessor are attached near the mastoid behind the patient's ear. Eight buffered electrodes are placed across the head at the location of interest. EEG data is collected and transmitted via BLE to a computer or smartphone for further processing.

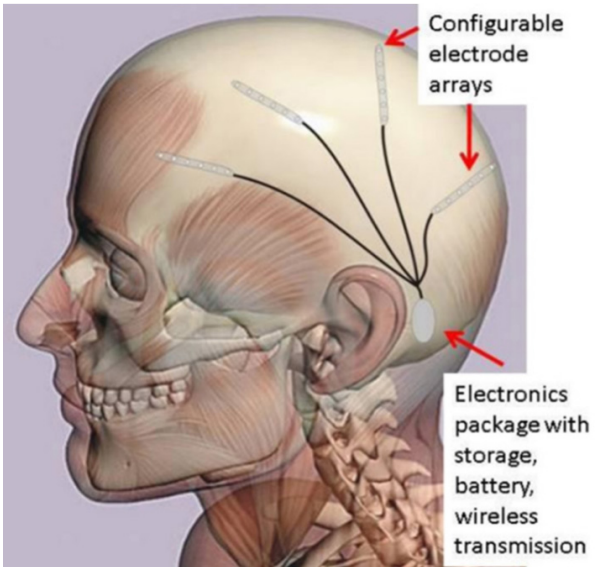

▲Figure 1: Implanted EEG system showing location of the SoC and electrodes.

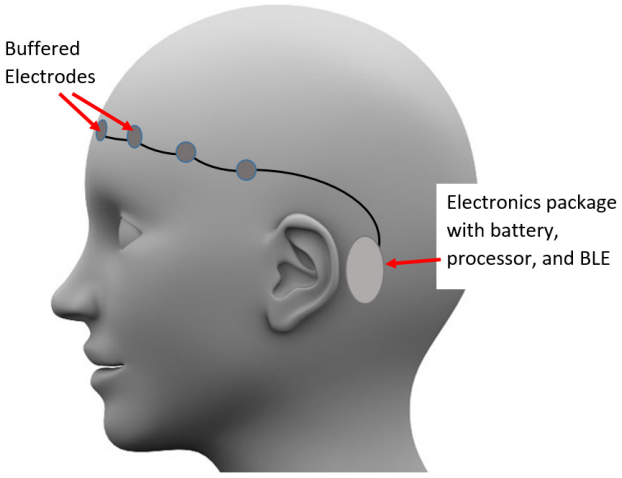

▲Figure 2: Wearable EEG system showing locations of electronics package and electrodes.

A Wearable Transcranial Doppler Ultrasound Phased Array System

S. J. Pietrangelo, H.-S. Lee, C. G. Sodini
Sponsorship: MEDRC, Maxim Integrated

The central objective of critical care for patients affected by traumatic brain injury (TBI), cerebrovascular accident (i.e., stroke), and other neurovascular pathologies is to monitor patient state and provide suitable medical intervention to mitigate secondary injury and aid in recovery. Transcranial Doppler (TCD) sonography is a specialized Doppler ultrasound technique that allows characterization of blood flow from the basal intracerebral vessels. While several non-invasive cerebrovascular diagnostic modalities exist, including positron emission tomography (PET), computed tomography (CT), and magnetic resonance angiography (MRA), the use of TCD sonography is highly compelling for certain diagnostic needs due to its safety in prolonged studies, high temporal resolution, modest capital equipment costs, and relative portability.

Despite a growing list of potential diagnostic applications, several constraints — notably operator-dependent measurement results, bulky instrumentation, and the need for manual vessel location — have generally confined the use of TCD ultrasound to highly specific clinical environments (e.g., neurocritical care units and vascular laboratories). This project seeks to develop a low-power miniaturized TCD ultrasound system for measuring blood flow velocity at the middle cerebral artery (MCA) in support of continuous cerebrovascular monitoring with limited operator interaction.

The TCD ultrasound system shown in Figure 1 employs multi-channel transceiver electronics and a two-dimensional transducer array to enable electronic steering of the ultrasound beam. The discrete prototype electronics measure 6.5" x 5.5" x 1" and are worn at the chest; the transducer array is affixed at the temporal region with an adjustable headframe. Electronic beam formation allows for algorithmic vessel location and tracking, thereby obviating the need for manual transducer alignment and operator expertise. Following automated vessel location, the system computes the flow velocity spectrogram and spectral envelope, as presented in Figure 2.

Although human validation is preliminary, this work demonstrates a compact, wearable, and algorithmically steered TCD system that largely resolves several key shortcomings of established TCD measurement techniques. The successful execution of our current objectives can profoundly alter the standard clinical approach to neurovascular evaluation, especially in applications where the role of non-invasive diagnostics has not yet been clearly established (e.g., extended monitoring, emergency assessment).

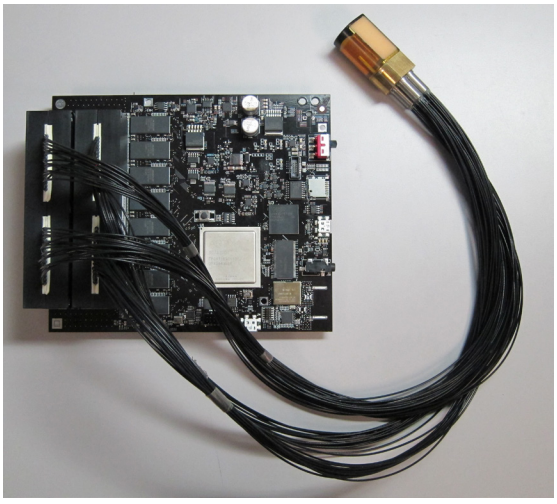

▲ Figure 1: Discrete TCD phased array system connected to a custom two-dimensional transducer array.

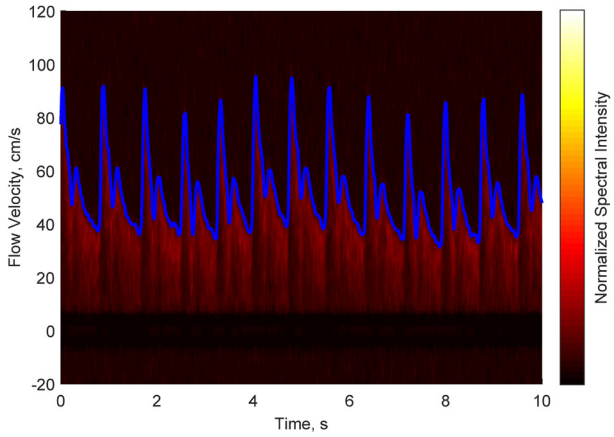

▲ Figure 2: TCD spectrogram at algorithmically located Doppler power maxima.

FURTHER READING

- S. J. Pietrangelo, "An Electronically Steered, Wearable Transcranial Doppler Ultrasound System," Master's thesis, Massachusetts Institute of Technology, Cambridge, 2013.

Continuous and Non-Invasive Arterial Pressure Waveform Monitoring Using Ultrasound

J. Seo, H.-S. Lee, C. G. Sodini
Sponsorship: Samsung Electronics Fellowship, MEDRC - Phillips

An arterial blood pressure (ABP) waveform provides valuable information for understanding cardiovascular diseases. The ABP waveform is usually obtained through a pressure transducer connected to an arterial catheter. Although considered the gold standard, this method has the disadvantage of its invasive nature. Non-invasive methods based on vascular unloading, such as Finapres, are not suitable for prolonged or continuous monitoring due to their obstructive nature. Therefore, reliable non-invasive ABP waveform estimation has been desired for a long time by medical communities. In that sense, medical ultrasound is an attractive imaging modality because it is inexpensive, free of ionizing radiation, cuff-less, and suitable for portable system implementation.

The proposed ultrasonic ABP waveform monitoring is achieved by observing the pulsatile change of the cross-sectional area and identifying the elastic property of the arterial vessel, represented by the pulse wave velocity (PWV; the propagation speed of a pressure wave along an arterial tree) with a diastolic blood pressure measurement as a baseline. The PWV can be estimated by obtaining a flow-area plot and then measuring the slope of a linear part in the flow-area plot during a reflection-free period (e.g., the early systolic stage).

A prototype ultrasound device is designed to obtain both a blood flow waveform and a diameter waveform simultaneously to implement the proposed technique, shown in Figure 1. A clinical test was conducted on nine healthy human subjects to demonstrate the proof of concept of the proposed approach. Figure 2 presents a pressure waveform comparison between an ABP waveform obtained at a left middle finger and an estimated ABP waveform at the left common carotid artery from this method. Currently, the prototype is being re-designed to reduce the data acquisition time in a clinical setting and potentially to enable device operation without the guidance of a sonographer.

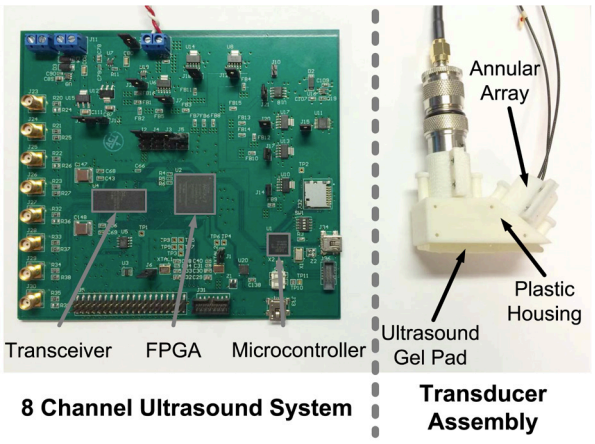

▲Figure 1: The prototype ultrasound system and transducer assembly. The system is capable of sufficient data rate to display blood flow and arterial pulsation simultaneously. Ultrasound gel pad is utilized to achieve acoustic coupling between the transducer surface and the skin.

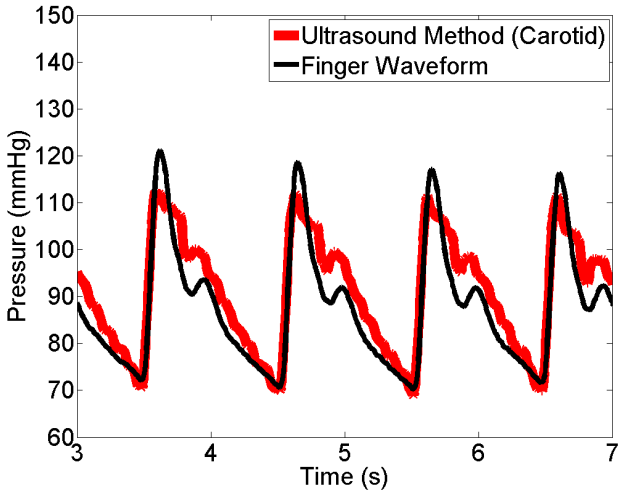

▲Figure 2: Comparison of the estimated carotid ABP waveform to the finger ABP waveform. The finger waveform shows a sharper systolic peak due to pulse pressure amplification at peripheral arterial sites.

FURTHER READING

- J. Seo, S. J. Pietrangelo, H.-S. Lee, and C. G. Sodini, "Carotid Arterial Blood Pressure Waveform Monitoring Using a Portable Ultrasound System," in *2015 37th Annual International Conference of the IEEE Engineering in Medicine and Biology Society (EMBC)*, pp. 5692-5695, 2015.
- J. Seo, S. J. Pietrangelo, H.-S. Lee, and C. G. Sodini, "Noninvasive Arterial Blood Pressure Waveform Monitoring Using Two-Element Ultrasound System," *IEEE Transactions on Ultrasonics, Ferroelectrics, and Frequency Control*, vol. 62, no. 4, pp. 776-784, 2015.

Improvement of a Capsule Endoscopic Ultrasound

D. Ibarra, J. H. Lee, B. W. Anthony
Sponsorship: Tecnológico de Monterrey, MIT

Wireless capsule endoscopy (WCE) has modernized the capacity for evaluation of the gastrointestinal (GI) tract. Even though WCE provides high-quality optical images of the GI tract, evaluation is restricted to the wall surface. This project studies design considerations for capsule endoscopic ultrasound (CEU) that combines the benefits of WCE and ultrasound imaging, enabling characterization of the deeper structures within the mucosal wall. The first part of the project has two goals: (1) to evaluate transducer designs and capsule materials appropriate for CEU and (2) to prove that the obtained ultra sound images have high-enough quality to work for us to design a wireless capsule. Mechanical scanning (MS) design is implemented using simulation and experimentation with a focused disc transducer and a motor. Measurements of 3-D printed phantoms were done using the TPX (4-methylpentene-1 based polyolefin) material for the capsule prototype. The MS-tethered capsule developed for imaging feasibility study shown in Figure 1(a) consists of a 10-MHz transducer and a micro stepper motor. Figure 1 (b) shows the first prototype with TPX material for the cover. A 3-D printed phantom was designed to evaluate image quality, and MS shows good performance in terms of image quality as well as system complexity. These findings support further development in the direction of a wireless capsule endoscopic ultrasound (WCEU) device with the goal of significantly expanding the diagnostic modalities for the GI tract.

Figure 2 (top) shows the 3-D printed phantom settled with a fishing line. Experimental results are shown in Figure 2 (bottom). Full circumferential coverage was done in a beaker of water with the capsule fitted in the 3-D printed phantom. The prototype acquires good B-mode images, the acoustic signal was stronger than expected due to the attenuation from the capsule wall. The further work is to test it in *in vivo* models to figure out the possibility of utilizing peristalsis such as acoustic coupling required for ultrasound imaging.

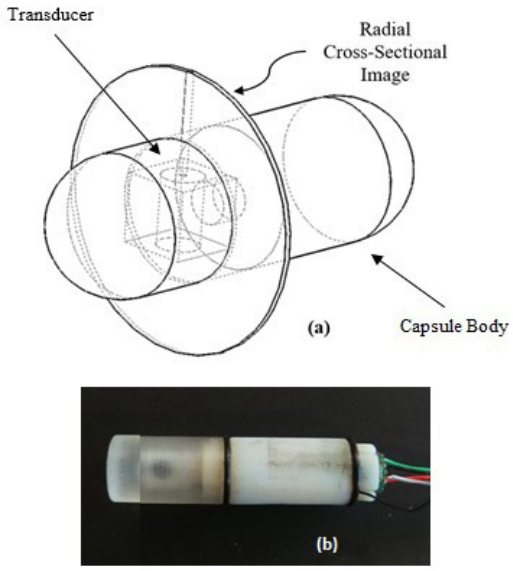

▲ Figure 1: The capsule design and the MS transducer rotated using a mechanical actuating element (a). The prototype of the capsule with cover of TPX material (b).

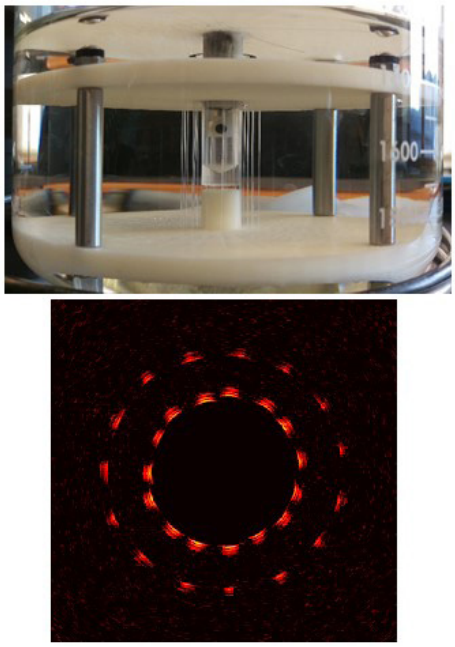

▲ Figure 2: The 3-D printed phantom settled with fishing line (top). The B-mode images of fishing line around 360° (bottom).

FURTHER READING

- J. H. Lee, G. Traverso, C. M. Schoellhammer, D. Blankschtein, R. Langer, K. E. Thomenius, D. S. Boning, and B. W. Anthony, "Towards Wireless Capsule Endoscopic Ultrasound (WCEU)," *2014 IEEE International Ultrasonics Symposium (IUS)*, pp. 734–737, 2014.
- L. B. Gerson, "Capsule Endoscopy and Deep Enteroscopy," *Gastrointest. Endosc.*, vol. 78, no. 3, pp. 439–443, September 2013.

Gastric Fluid-Activated Battery for Powering Ingestible Electronics

P. Nadeau, D. El-Damak, D. Glettig, S. Mo, C. Cleveland, L. Booth, R. Langer, A. P. Chandrakasan, G. Traverso
Sponsorship: Texas Instruments, Hong Kong Innovation and Technology Commission, ATIC-SRC Center of Excellence for Energy Efficient Electronics Systems, Alexander von Humboldt-Stiftung Foundation, National Institutes of Health

Ingestible electronics are revolutionizing the way we diagnose and treat diseases. Swallowable telemetry capsules are now used to take visual images of the gastrointestinal (GI) tract, record vital signs, and monitor temperature, pH, and medication compliance. In addition, techniques for longer-term gastric residency (up to 1 week) are extending the lifetime of ingestible devices and could provide a platform for longer term monitoring (Figure 1).

With the scaling of CMOS power consumption, primary cell batteries may not be the only option for powering these devices. Dissolving electrodes made from biocompatible materials could provide a safe and potentially lower cost solution for powering ingestible electronic sensors (Figure 2). In these electrochemical cells, the gastric fluid acts as the electrolyte and activates the battery on contact. The anode metal (either zinc or magnesium) dissolves into the acid while the inert cathode catalyzes the evolution of hydrogen gas, sending electrical power to the circuit.

The focus of this research includes the detailed un-tethered (wireless) characterization of the available amount of power from such an electrochemical cell as it traverses the GI tract, including such parameters as the electrode voltages and impedance levels. Due to food and fluid intake, the heterogeneous nature of the gastric pool, and varying position of the capsule within the stomach due to motion, the available amount of power is expected to have large variability. Understanding this variation can provide valuable input for system designers. As a first step we are gathering preliminary data on the *in vivo* performance of this cell in a large animal model. In addition to characterization, we seek to harness this energy to demonstrate fully self-powered measurements and wireless communication to an external base station receiver.

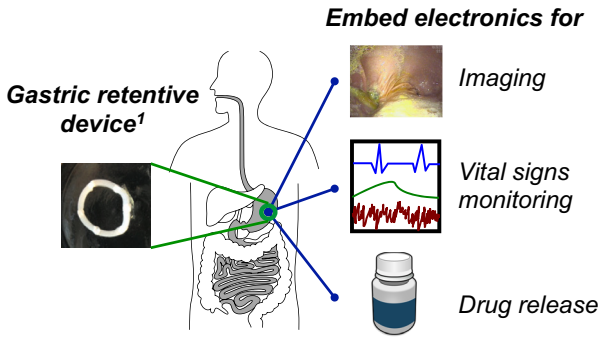

▲ Figure 1: Gastric retentive devices as a platform for health monitoring and treatment.

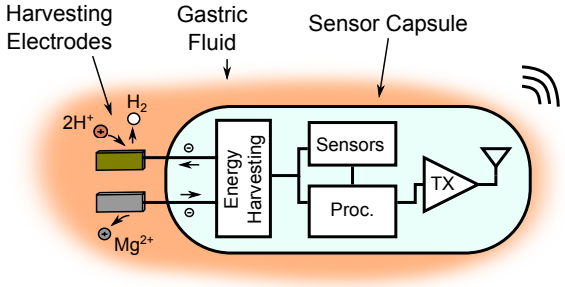

▲ Figure 2: Electronic device powered by harvesting from electrodes which are activated by gastric fluid.

FURTHER READING

- S. Zhang, A. M. Bellinger, D. L. Glettig, R. Barman, Y.-A. L. Lee, J. Zhu, C. Cleveland, V. A. Montgomery, L. Gu, L. D. Nash, D. J. Maitland, R. Langer, and G. Traverso, "A pH-Responsive Supramolecular Polymer Gel as an Enteric Elastomer for Use in Gastric Devices," *Nature Materials*, vol. 14, no. 10, pp. 1065–1071, July 2015.
- G. Traverso, G. Ciccarelli, S. Schwartz, T. Hughes, T. Boettcher, R. Barman, R. Langer, and A. Swiston, "Physiologic Status Monitoring via the Gastrointestinal Tract," *PLoS ONE*, vol. 10, no. 11, pp. e0141666, 2015.

High-Throughput Cell Sorting for Diagnostics using Microfluidics

M. Kim, K. Choi, H. Ryu, W. Ouyang, J. Han in collaboration with D. T. Hung, G. Alter, J. Lee, B. Levy
Sponsorship: NIH, Broad BN10, J-WAFS

Our group is collaborating on high-throughput cell and molecular sorting, often from challenging sample backgrounds such as blood or sputum, to enable advanced, functional assays and diagnostics. One of the common challenges in biomedical sciences is reliable sample preparation, and there are many situations where better sample preparation (which involves removal of backgrounds and concentration of target cells or molecules) can drastically enhance the sensitivity and specificity of the downstream assays.

As one of the main applications, we are focusing on bacterial sorting from blood to enable blood-borne pathogen diagnostics. Bacterial contamination and infection are a significant problem for public health, food industry, environmental biosafety, and many other areas. However, current techniques do not allow rapid and sensitive detection of bacteremia that are necessary for better clinical management. To address this problem, we developed a method to rapidly isolate bacteria from whole blood using inertial microfluidics and directly determine pathogen identity and antibiotic susceptibility with hybridization-based RNA detection. The Dean Flow Fractionation (DFF) cell-sorting technology described here and applied to bacterial isolation was previously developed by our group for direct isolation of circulating tumor cells (CTCs) from whole blood. Unlike CTCs that exhibit 10–20 μm characteristic length, bacteria (<1 μm) are significantly smaller and therefore challenging to focus using conventional inertial microfluidics. To overcome the size problem, we introduced a sheath flow at the inlet to "pinch" the bacteria-containing sample and demonstrated well-controlled Dean migration of bacteria towards the outer wall to achieve efficient bacteria recovery. Using the DFF principle, bacteria are separated from host blood cells in a label-free separation method with high recovery, even in low abundance bacteria situation. Ribosomal RNA detection can then be applied for direct identification of low abundance pathogens (~100 mL^{-1}) from blood without culturing or enzymatic amplification. Messenger RNA detection of antibiotic-responsive transcripts after brief drug exposure permits rapid susceptibility determination from bacteria with minimal culturing (~10^5 mL^{-1}). This novel combination of microfluidic cell separation with RNA-based molecular detection techniques represents significant progress towards faster diagnostics (~8 hours) to guide antibiotic therapy.

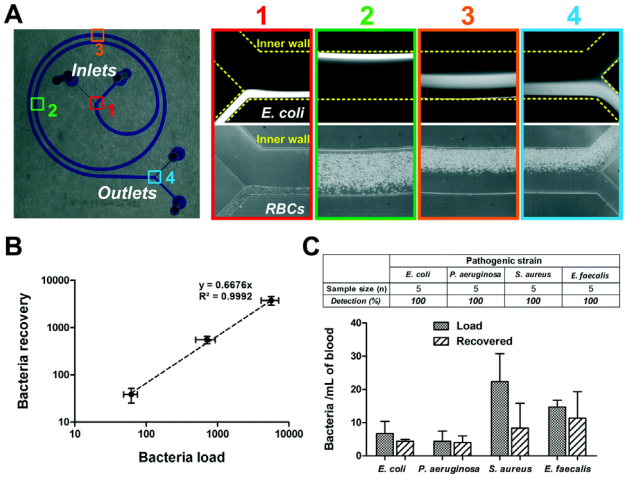

▲ Figure 1: (A) Distribution of FITC-labeled E. coli and RBCs shows their differences along the separation channel. (B) Recovery plot indicates efficient bacterial recovery (>65%). (C) Histogram plot indicates the bacterial load and recovery for different pathogenic strains at clinically relevant concentrations (~10–50 cells mL^{-1}).

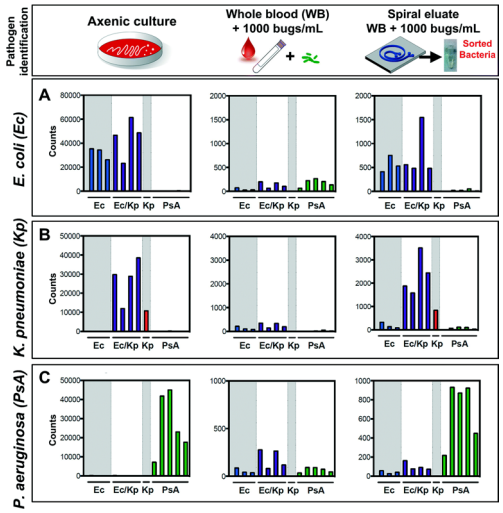

▲ Figure 2: Pathogen identification from blood after DFF by rRNA recognition. (A) E. coli or (B) K. pneumoniae were either grown in axenic culture (left panel); in whole blood (middle); or in DFF-processed whole blood (right), before being detected by the NanoString assay using a probeset directed against rRNA from these three organisms.

FURTHER READING

- H. W. Hou, R. P. Bhattacharyya, D. T. Hung, and J. Han, *Lab on a Chip*, vol. 15, pp. 2297-2307, 2015.
- D. Di Carlo, D. Irimia, R. G. Tompkins, and M. Toner, *Proc. Natl. Acad. Sci. U. S. A.*, vol. 104, pp. 18892–18897, 2007.
- H. W. Hou, M. E. Warkiani, B. L. Khoo, Z. R. Li, R. A. Soo, D. S.-W. Tan, W.-T. Lim, J. Han, A. A. S. Bhagat, and C. T. Lim, *Sci. Rep.*, vol. 3, pp. 1259, 2013.

Nanofluidic Devices for Biologics Quality Assessment

S. H. Ko, W. Ouyang, T. Kwon, J. Han
Sponsorship: Integrated and Scalable Cyto-Technology Platform for Biopharmaceutical Manufacturing on Demand Project /DARPA

Biologics (protein drugs), which are applicable to the most effective means to treat serious diseases, are of great interest in the modern pharmaceutical industry. However, assuring their quality and safety is more difficult than it is for small molecule drugs due to their high sensitivity to external environment conditions, so developing analytical tools for exact and rapid quality assessment is essential. In this work, we have designed nanofluidic devices and demonstrated purity and bioactivity assessments for commercialized biologics using size-based separation and mobility-shift assay methods.

For the purity assessment, a slanted nanofilter array is used to demonstrate separation of the target (human growth hormone, or hGH) and impurities (molecular weight markers) based on size to reveal the presence of protein aggregation (potential cause of immune responses *in vivo*) or any fragments. Figure 1 shows the analysis of hGH with impurities. The device could resolve all the impurities although the low-molecular weight impurities (14.3 kDa and 3.5 kDa proteins) are not fully resolved. The bioactivity assessment is achieved by using positively modulated receptor as a probe molecule (growth hormone receptor or GHR(+)) to perform direct assay for assessing binding affinity (k_D). While GHR(+) is not concentrated, the complex GHR(+)-hGH is concentrated, with a stronger signal at higher hGH concentrations. Based on the fluorescence intensity of concentrated complex, the dose-response curve is plotted, indicating an apparent k_D of 1 nM, as shown in Figure 2.

The nanofluidic devices developed here have potential for drug (biologics) analysis. The devices have several advantages over conventional analytical tools, such as short operational time (less than 1 hour), operational simplicity, and small sample volume. Therefore, the nanofluidic devices are applicable for assuring quality and safety of biologics rapidly as point-of-care monitoring system.

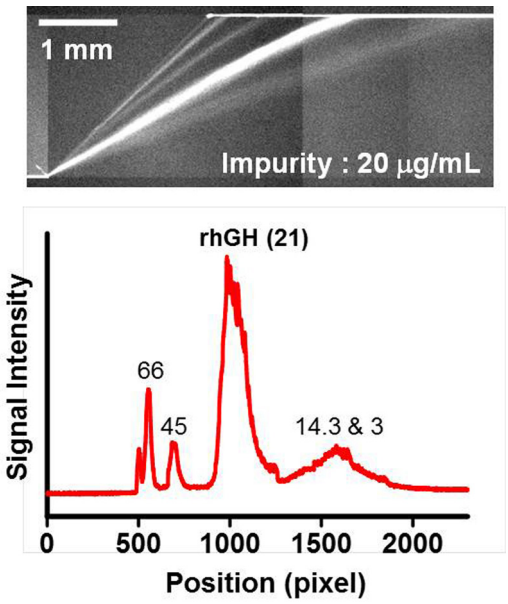

▲Figure 1: Demonstration of purity assessment of hGH with molecular weight markers to simulate impurities using size-based separation (all samples are denatured by SDS, and the unit of molecular weight is kDa). Fluorescence profiles are measured along white dot line.

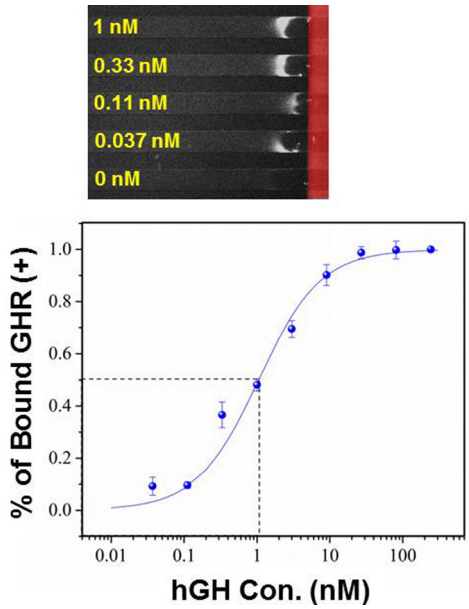

▲Figure 2: Mobility-shift homogeneous assay for bioactivity assessment for hGH via receptor. The dose-response curve depending on hGh concentration shows 1 nM of k_D.

FURTHER READING

- S. H. Ko, W. Ouyang, D. Chandra, A. Y. Wang, P. Karande, W. Hancock, and J. Han, "A Nanofluidic Device for Rapid Biologics Quality Control," *Proc. 19th International Conference on Miniaturized Systems for Chemistry and Life Sciences*, Gyeongju, South Korea, pp. 329-331, 2015.
- W. Ouyang, S. H. Ko, A. Y. Wang, W. Hancock, and J. Han, "A Versatile Platform for Rapid Biologics Activity Assessment via Microfluidic Drug-Receptor Binding Assays," in *Proc. 19th International Conference on Miniaturized Systems for Chemistry and Life Sciences*, Gyeongju, South Korea, pp. 928-930, 2015.

Measuring Absolute Concentration of Particles in Suspension Using High Frequency B-mode Ultrasound Imaging

J. H. Lee, B. W. Anthony, D. S. Boning
Sponsorship (in part): Madrid-MIT M+Visión Consortium

Measuring particle concentration is one of the most essential procedures in life sciences, routinely performed in research laboratories as well as in clinics. For example, counts of blood cells are important parameters included in almost all blood tests. Several methods are available for measuring particle concentration. The most often used involves a hemocytometer, where the sample is placed in a chamber of known volume and particles are counted under an optical microscope. While the existing methods work well, they are not without limitations. One weakness is that the volumes analyzed by these methods are typically small. This limitation is especially problematic when the concentration is low because small analysis volumes lead to insufficient counts, which increases the measurement error. In addition, these methods are typically destructive in that the analyzed sample cannot be retrieved, which limits the volume that can be analyzed.

This work proposes an ultrasound-based concentration measurement method intended for dilute samples of micron-scale particles. Unlike the existing ultrasound-based methods, the proposed method is based on detecting individual particles in order to produce a direct particle count. It has been shown that when the scatterer size is similar to the wavelength of the ultrasound, individual scatterers can be distinguished in the B-mode image. While the number of scatterers in the image can be counted relatively easily, attaining the exact volume analyzed by the image as required to calculate the absolute concentration is not straightforward because the slice thickness of the image is unknown. The proposed method estimates the volume of a B-mode ultrasound image by examining the lateral spreading of individual echoes. In addition, by characterizing the backscatter coefficient of the echoes, this method can classify the different particle types and measure their concentrations separately. The method is entirely image-based and does not require prior characterization of the sample.

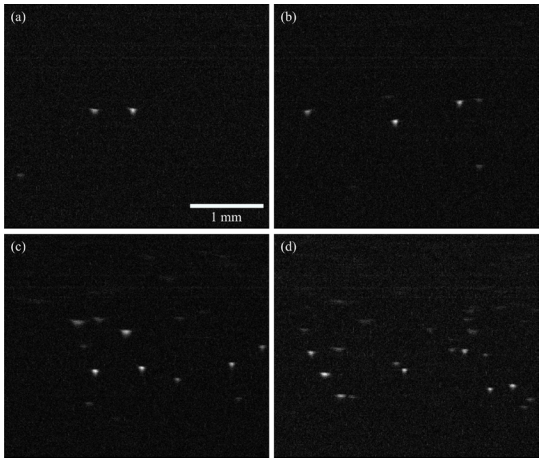

▲Figure 1: B-mode ultrasound images of 10 μm polystyrene microspheres suspended in distilled water. (a) 5 particles/μL, (b) 10 particles/μL, (c) 20 particles/μL, and (d) 50 particles/μL.

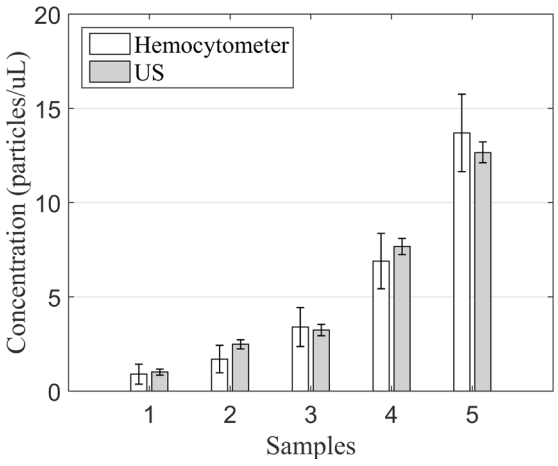

▲Figure 2: Concentration measurement results. The results from the proposed method are compared with reference measurements made with a Fuchs-Rosenthal hemocytometer.

FURTHER READING

- J. H. Lee, J. Jiménez, X. Zhang, D. S. Boning, and B. W. Anthony, "Ultrasound Image-Based Absolute Concentration Measurement Technique for Materials with Low Scatterer Concentration," presented at *2015 IEEE International Ultrasonics Symposium (IUS)*, Taipei, Taiwan, 2015.
- R. E. Baddour, M. D. Sherar, J. W. Hunt, G. J. Czarnota, and M. C. Kolios, "High-Frequency Ultrasound Scattering from Microspheres and Single Cells," *The Journal of the Acoustical Society of America*, vol. 117, no. 2, pp. 934–43, 2005.
- K. P. Mercado, M. Helguera, D. C. Hocking, and D. Dalecki, "Estimating Cell Concentration in Three-Dimensional Engineered Tissues Using High Frequency Quantitative Ultrasound," *Annals of Biomedical Engineering*, vol. 42, no. 6, pp. 1292–1304, 2014.

High-Speed Multiple-Mode Mass Sensing Resolves Dynamic Nanoscale Mass Distributions

S. Olcum, N. Cermak, S. C. Wasserman, S. R. Manalis
Sponsorship: U.S. Army Research Office, NCI

Simultaneously measuring multiple eigenmode frequencies of nanomechanical resonators can determine the position and mass of surface-adsorbed proteins and could ultimately reveal the mass tomography of nanoscale analytes. However, existing measurement techniques are slow (<1 Hz bandwidth), limiting throughput and preventing use with resonators generating fast transient signals. We develop a general platform for independently and simultaneously oscillating multiple modes of mechanical resonators (Figure 1), enabling frequency measurements that can precisely track fast transient signals within a user-defined bandwidth that exceeds 500 Hz. We use this enhanced bandwidth to resolve signals from multiple nanoparticles moving simultaneously through a suspended nanochannel resonator and show that four resonant modes are sufficient for determining their individual position and mass with an accuracy near 150 nm and 40 attograms throughout their 150 ms transit (Figure 2). We envision that our method can be readily extended to other systems to increase bandwidth, numbers of modes, or number of resonators.

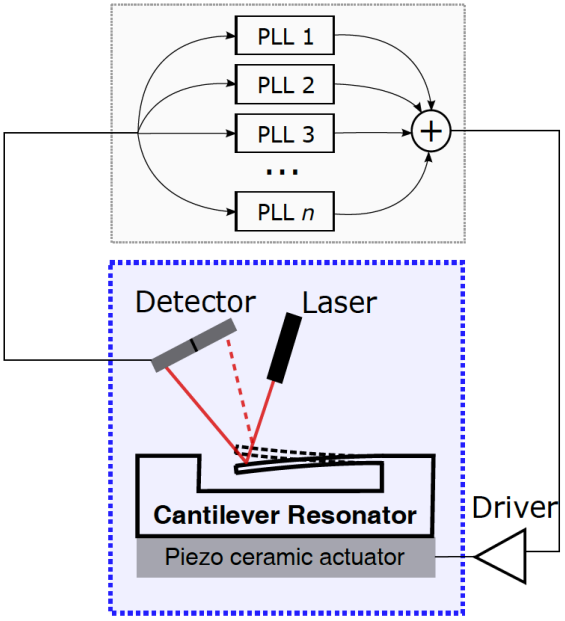

▲Figure 1: Schematic representation of the multi-mode resonator system operating in closed loop with multiple phase lock loops (one per resonant mode).

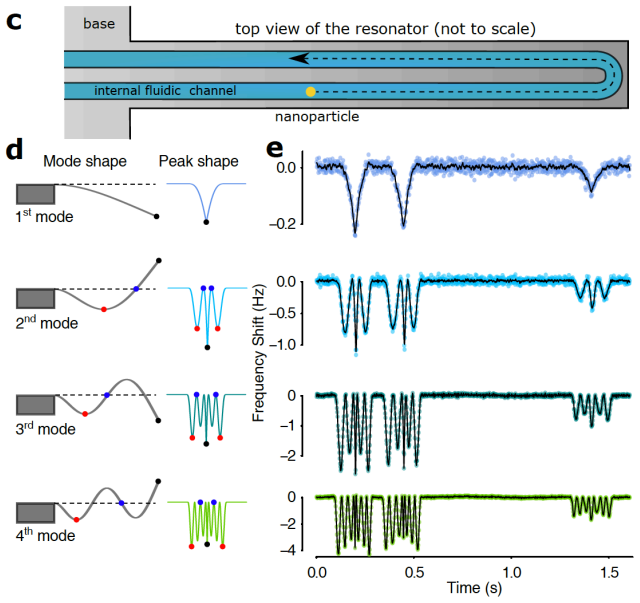

▲Figure 2: Schematic showing internal channel of resonator and bending profiles of first four resonant modes along with corresponding frequency deviations when particle with constant velocity travels through resonator. Bottom right shows frequency measurements of first four bending modes as two 150-nm and one 100-nm gold nanoparticle transit through resonator.

FURTHER READING

- S. Olcum N. Cermak S. C. Wasserman, and S. R. Manalis, "High-Speed Multiple-Mode Mass-Sensing Resolves Dynamic Nanoscale Mass Distributions," *Nature Communications*, vol. 6, pp. 7070, 2015.

Expansion Mini-Microscopy for the Identification of Pathogenic Bacteria

Y. S. Zhang, J.-B. Chang, M. M. Alvarez, G. Trujillo-de Santiago, J. Alemán, B. Batzaya, V. Krishnadoss, A. A. Ramanujam, M. Kazemzadeh-Narbat, F. Chen, P. W. Tillberg, M. R. Dokmeci, E. S. Boyden, A. Khademhosseini
Sponsorship: MIT-Tecnológico de Monterrey Nanotechnology Program, CONACyT, Fundación México en Harvard

Regretfully, even a modest but good optical microscope is frequently unavailable and unaffordable in remote and underprivileged areas. Expansion mini-microscopy (ExMM) is a novel form of microscopy, recently developed by our groups, in which specimens are physically (as supposed to optically) expanded and then observed by means of a low-cost mini-microscope (basically, a web camera with an inverted lens). Expansion microscopy and mini-microscopy have both been validated in different contexts. The technique of expansion microscopy was first introduced by Ed Boyden's group for physical expansion of human cells. Mini-microscopy was first introduced by Ali Khademhosseini´s group. The integration of these technologies is straightforward and will result in a simple and portable, but powerful and reliable diagnostic tool.

We are developing ExMM techniques to observe and identify common life-threatening pathogens. So far, Escherichia coli, a common cause of diarrhea in children and neonatal sepsis, has been taken as our first proof-of-principle model. In brief, ExMM can process a tissue or blood sample in successive steps. First, the sample is embedded in a polymeric pre-gel containing specific antibodies directed to the target pathogen (Figure 1A); a secondary antibody marked with a fluorophore and containing a covalently attached small DNA sequence is directed against the heavy chain of the primary antibody (Figure 1B); and monomers, containing a DNA complementary sequence (blue) (Figure 1C). The sample is trapped within the polymeric matrix by a photo-induced crosslinking reaction and then degraded with a proteinase enzyme, leaving the skeleton tagged with antibodies (or antibody fragments). Expansion of the polymeric matrix is achieved by addition of water and the structure defined by the fluorophores expand isotropically. The expansion is selective, meaning that only the surfaces tagged with antibodies (suspected pathogen) will expand. Finally, the sample is observed through a simple, inexpensive (~20 USD), and portable mini-microscope. Since specific antibodies can be used against different pathogens (i.e. E. coli can be antibody-marked in green and Streptococcus spp in red), the technique can conclusively and unequivocally identify the causative agent of an infection further facilitating proper intervention. More importantly, the technique does not require a trained microscopist or an expensive bench-top microscope, so we believe it will simplify, expedite, and improve the accuracy of diagnosis worldwide, and particularly in remote and underdeveloped regions.

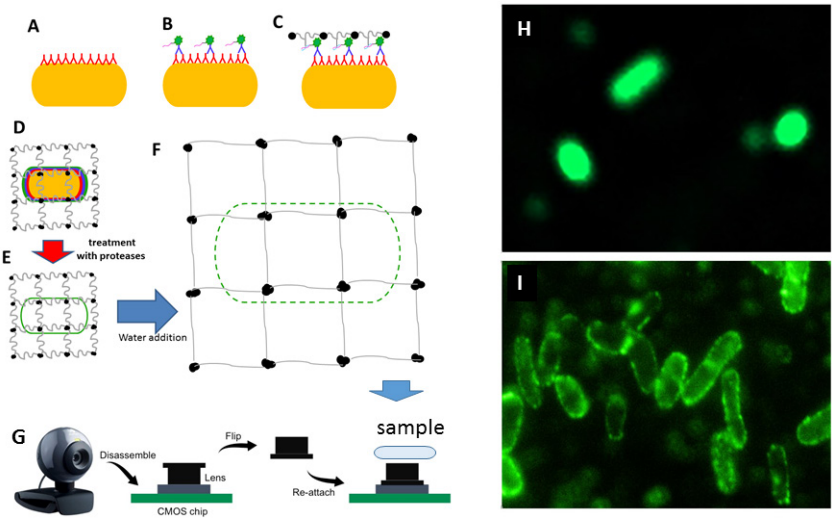

◀Figure 1: ExMM: (A) A pathogen is tagged with specific primary antibodies (red), (B) and secondary antibodies marked with a fluorophore (blue-green) and containing a small DNA sequence (pink). (C) The addition of monomers containing a DNA complementary sequence (blue), completes the expansion mix. (D) The sample is trapped within the polymeric matrix by photo-induced crosslinking. (E) Proteases are added to degrade the sample and the antibodies. (F) Expansion of the polymeric matrix is achieved by addition of water. (G) The mini-microscope is constructed by inverting the lens of a commercial web-camera. Images of *E. coli* captured with a benchtop microscope (H) before expansion, and (I) after expansion.

FURTHER READING

- F. Chen, P. W. Tillberg, and E. S. Boyden, "Expansion Microscopy," *Science*, vol. 19, pp. 543-548, January 2015.
- Y. S. Zhang, Y. S. Zhang, J.-B. Chang, M. M. Alvarez, G. Trujillo-de Santiago, J. Alemán, B. Batzaya, V. Krishnadoss, A. A. Ramanujam, M. Kazemzadeh-Narbat, F. Chen, P. W. Tillberg, M. R. Dokmeci, E. S. Boyden, and A. Khademhosseini, "Hybrid Microscopy: Enabling Inexpensive High-Performance Imaging through Combined Physical and Optical Magnifications," *Scientific Reports*, vol. 6, pp. 22691:1-10, March 2016.

High-Efficiency Capture of Pathogens in Chaotic Flows

G. Trujillo-de Santiago, G. Prakash, A. Risso, P. I. Sánchez-Rellstab, Y. S. Zhang, M. M. Alvarez, A. Khademhosseini
Sponsorship: MIT-Tecnológico de Monterrey Nanotechnology Program, CONACyT, Fundación México en Harvard

Infectious diseases, both of viral and bacterial origin, continue to be a health threat to millions of people in developed and underdeveloped countries. In cases of sepsis or viral infections such as Ebola disease and HIV, effective capture and removal of the pathogenic agent from the bloodstream is one potentially successful treatment strategy (i.e., pathogen blood cleansing). We are developing filter-less technologies for the direct capture of *Escherichia coli* (as a model pathogen) from the bloodstream. In a later stage of this project, we will work on the capture of viruses (i.e., Ebola virus-like-particles) using an analogous approach.

Our strategy is simple: We use a portable/disposable system for the continuous capture of bacterial particles circulating through a microfluidic chamber. The system is based on the specific recognition of proteins on *E. coli* membranes; it integrates the use of (a) anti-*E. coli* polyclonal antibodies, (b) magnetic nanoparticles (MNP), (c) a microfluidic chaotic flow system, and (d) a neodymium magnet. Anti-*E. coli* antibodies are covalently immobilized within commercial magnetic nanoparticles to fabricate nanoparticles that will bind *E. coli* bacteria (Figure 1B). Our experiments compare the performance of different immobilization strategies (amino-carboxylic covalent binding and streptavidin-biotin binding) and different magnetic nanoparticle sizes (range 30–800 nm). The heart and distinctive feature of our system is a microfluidic chamber where the *E. coli* binding particles and the bacteria are mixed by the action of a laminar chaotic flow produced by the alternating rotation of two cylinders (Figure 1C). The intimate contact induced by this chaotic laminar flow promotes bacteria capture by individual nanoparticles or nanoparticle clusters (Figure 1D). The trapped *E. coli* are concentrated by a simple magnet located downstream from the microchamber (Figure 1E).

This platform has key advantages over currently available methods, which are mostly based on the use of microfluidic channels or filtering membranes: (a) It is faster (overall capture times in the order of 1–5 minutes); (b) It offers superior capture due to the intimate mixing induced by the chaotic flow; (c) It is easy to use, which reduces labor efforts and eliminates the need for dedicated and costly infrastructure.

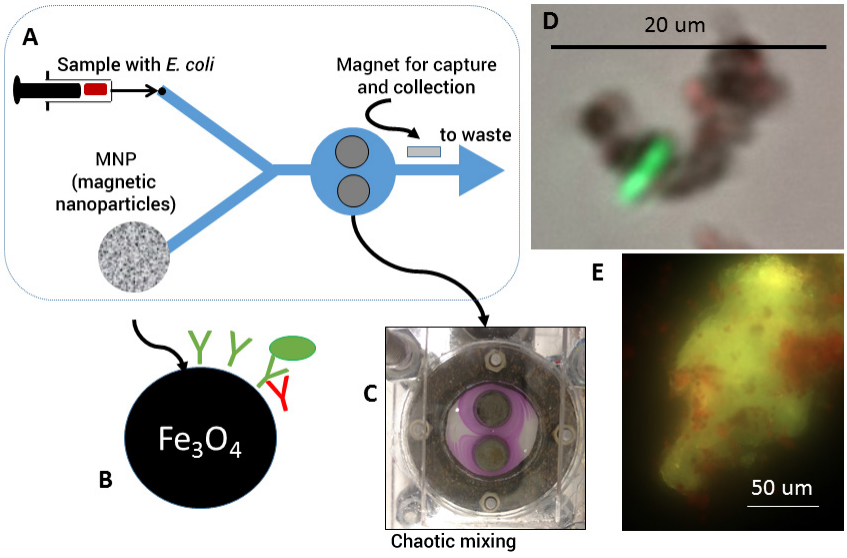

◀ Figure 1: Our pathogen capture system integrates magnetic nanoparticles (MNPs) functionalized with antibodies, a microfluidic chaotic chamber, and a static magnet. (A) General scheme. A sample spiked with *E. coli* bacteria is mixed with (B) MNPs functionalized with anti-*E. coli* antibodies (green Y). The presence of anti-*E.coli* antibodies can be validated by marking with a secondary antibody (red Y). (C) Mixing of the functionalized MNPs and the bacteria occurs under the action of a chaotic flow induced by the alternating rotation of two cylinders. (D) Zoomed view of a bacterium captured in an MNP cluster. (E) The action of the magnet concentrates the bacteria-loaded MNPs.

FURTHER READING

- WHO. Fact Sheets. "Infectious Diseases." [Online]. Available: http://www.who.int/topics/infectious_diseases/factsheets/en/.

Magnetic Nanoparticles for Wireless Manipulation of Neural Circuits

R. Chen, M. G. Christiansen, C. Loynachan, G. Romero, A. W. Senko, P. Anikeeva
Sponsorship: NSF, DARPA

Weak magnetic susceptibility and conductivity of biological matter suggest the application of alternating magnetic fields (AMF) with low amplitudes (~1-10s mT) and frequencies in the 100-kHz range for delivery of signals into deep-tissue targets. One can use nanomaterial transducers to convert the externally applied AMF into biological stimuli such as mechanical deformation or thermal perturbation. The latter can be achieved by magnetic nanoparticles 5-30 nm in diameter composed of biochemically stable and benign ferrites, such as iron oxide. When exposed to AMF with the abovementioned parameters, these MNPs undergo magnetization reversal, and the resulting hysteretic power loss is dissipated as heat.

Guided by the dynamic hysteresis model, we have previously engineered a palette of ferrites and identified the AMF conditions leading to high heating efficiencies in these nanomaterials. We have then applied the concept of magnetothermal stimulation to two biological systems: wireless excitation of neural activity and remote disaggregation of amyloid beta (Aβ) deposits characteristic of Alzheimer's disease. To enable AMF-driven neural excitation, we took advantage of a heat sensitive calcium channel TRPV1 (a capsaicin receptor), which is broadly expressed across the nervous system. We found that exposure to AMF in the presence of MNPs triggers TRPV1 and the corresponding influx of calcium ion into neurons leading to action potential firing (Figure 1). Externally controlled disruption of ~10-μm–sized Aβ aggregates into ~100s-nm fragments was observed when MNPs specifically targeted to Aβ via a coating with a short peptide (LPFFD) were exposed to AMF for 3-6 hrs (Figure 2).

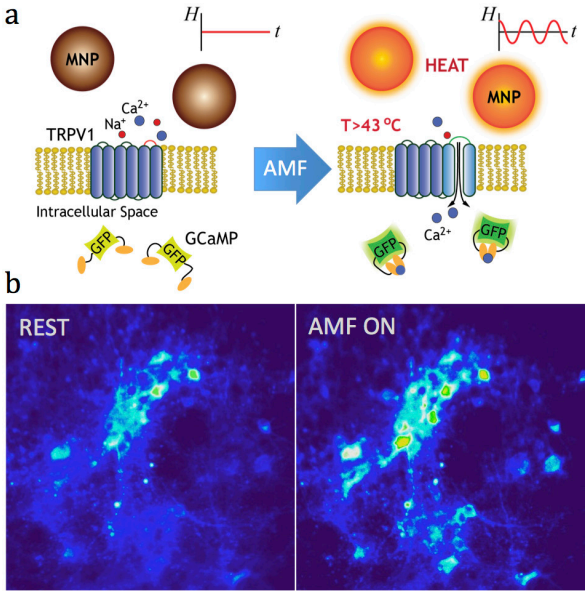

▲ Figure 1: (a) Magnetothermal stimulation schematic. MNP = magnetic nanoparticle; TRPV1 = heat sensitive (calcium) ion channel; AMF = alternating magnetic field; GFP = green fluorescent protein; GCaMP6 = fluorescent calcium ion indicator. (b) AMF evokes activity in neurons in the presence of MNPs as recorded by GCaMP6 fluorescence increase.

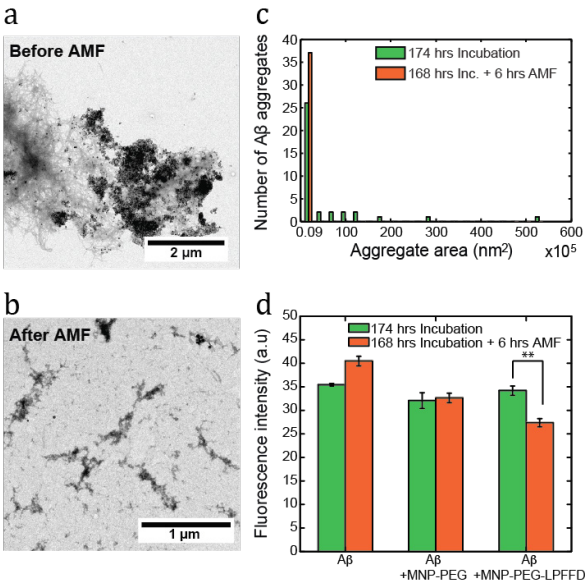

▲ Figure 2: (a) Amyloid beta (Aß) aggregate decorated with MNPs. (b) Aggregate dissociated by magnetothermal stimulus transduced by MNPs. (c) Size distribution of aggregates as measured by transmission electron microscopy with and without exposure to AMF. (d) Fluorescence of the Aß stain thioflavin T indicates disruption of aggregates using targeted MNPs. PEG = poly(ethylene glycol); LPFFD = targeting peptide.

FURTHER READING

- R. Chen, M. G. Christiansen, and P. Anikeeva, "Maximizing Hysteretic Losses in Magnetic Ferrite Nanoparticles via Model-Driven Synthesis and Materials Optimization," *ACS Nano*, vol. 7, pp. 8990-9000, 2013.
- R. Chen, G. Romero, M. G. Christiansen, A. Mohr, and P. Anikeeva, "Wireless Magnetothermal Deep Brain Stimulation," *Science* 347, pp. 1477-1480, 2015.
- C. N. Loynachan, G. Romero, M. G. Christiansen, R. Chen, R. Ellison, T. T. O'Malley, U. P. Froriep, D. M. Walsh, and P. Anikeeva, "Targeted Magnetic Nanoparticles for Remote Magnetothermal Disruption of Amyloid-β Aggregates," *Adv. Health. Mater.*, vol. 4, pp. 2100-2109, 2015.